Journal of Food Bioactives
International Society for Nutraceuticals and Functional Foods
Original Research
J. Food Bioact. 2023;22:43–52

Protective effect of *Melanogrammus aeglefinus* skin oligopeptide in ultraviolet B-irradiated human keratinocytes

Ziyan Wang[a,b], Lisha Dong[b], Jiaojiao Han[a,b], Jun Zhou[a,b], Chenyang Lu[a,b], Ye Li[a,b], Tinghong Ming[a,b], Zhen Zhang[a,b], Rixin Wang[b*] and Xiurong Su[a,b*]

[a]State Key Laboratory for Quality and Safety of Argo-products, Ningbo University, Ningbo 315211, China
[b]School of Marine Science, Ningbo University, Ningbo 315832, China
[*]**Corresponding author:** Rixin Wang and Xiurong Su, School of Marine Science, Ningbo University, 169 Qixing South Road, Ningbo 315832, China. E-mail: wrx_zjou@163.com and suxiurong_public@163.com
DOI: 10.31665/JFB.2023.18347
Received: June 02, 2023; **Revised received & accepted:** June 17, 2023
Citation: Wang, Z., Dong, L., Han, J., Zhou, J., Lu, C., Li, Y., Ming, T., Zhang, Z., Wang, R., and Su, X. (2023). Protective effect of *Melanogrammus aeglefinus* skin oligopeptide in ultraviolet B-irradiated human keratinocytes. J. Food Bioact. 22: 43–52.

Abstract

Ultraviolet B (UVB)-induced cell death causes skin photoaging. In this study, we investigated the protective effect of *Melanogrammus aeglefinus* skin oligopeptide (MSOP) in UVB-irradiated human keratinocytes. The method of preparing MSOP was optimized, and three peptides with high abundance, VADML (Val-Ala-Asp-Met-Leu), IARF (Ile-Ala-Arg-Phe) and SSPSF (Ser-Ser-Pro-Ser-Phe), were identified. Discovery Studio predicted that these peptides interacted with Keap1 and contributed to antioxidant activity. Therefore, a UVB-induced cell model was used to explore the beneficial effects of MSOP *in vitro*. The activities of superoxide dismutase and glutathione peroxidase were increased in the MSOP-treated groups, while the malondialdehyde content was decreased. In addition, 23 differentially expressed proteins were identified through quantitative proteomics analysis; among them, the upregulation of Nrf2 and downregulation of Keap1, which are involved in the Keap1/Nrf2/ARE signaling pathway, contributed to the antioxidant process. Based on this study, MSOP might be an alternative agent for protecting the skin against UVB exposure.

Keywords: *Melanogrammus Aeglefinus* skin oligopeptide; Ultraviolet B; Photic damage; Antioxidation; Quantitative proteome.

1. Introduction

Exposure to excessive sunlight is an important etiologic factor in the development of acute inflammation and is thus consequently linked to the progression of skin cancer (Hooda et al., 2023). Ultraviolet B (UVB) is the most damaging component of solar radiation that reaches the earth and is a major risk factor for the development of acute inflammation as well as nonmelanoma skin cancer in the epidermis (Lim et al., 2022). When the skin is exposed to UV light, a photooxidative reaction is initiated that impairs the antioxidant status and increases the cellular level of reactive oxygen species (ROS) (Kumar et al., 2022; Masaki et al., 2009). This process, which is commonly known as photoaging, impairs the self-protection property of the skin and consequently damages the cutaneous tissues (Berry et al., 2022).

Skin aging is a complex phenomenon that results from interactions between intrinsic and extrinsic factors. Intrinsic or chronological aging is an inevitable, genetically programmed process related to a natural decline in the normal physiological process whereas extrinsic aging is caused by environmental factors (Löwenau et al., 2017; Uitto, 1997). Both intrinsic and extrinsic factors are superimposed in sun-exposed areas of skin, resulting in marked histological changes in the extracellular matrix (ECM); clinically, the changes are observed as, photoaged skin with loss of rigidity and elasticity (Freitas-Rodríguez et al., 2017; Oh et al., 2020). Antioxidants have the capability to quench ROS and have been reported to repair skin damage, loss of elasticity, wrinkling and premature aging when supplemented in the diet (Fernandes et al., 2023; Liu, et al., 2023). Thus, it is suggested that regular consumption of antioxidant-containing natural ingredients might be a useful strategy for protection against

UV-mediated cutaneous damage.

Cod is among the most important commercial food species used worldwide, and a large amount of byproduct is generated during processing. Skin is a good source of collagen, which accounts for 8% of the byproduct (Bruno Siewe et al., 2021; Chen et al., 2020). It has been reported that cod skin oligopeptide induces apoptosis and leads to inhibition of human gastric carcinoma cell growth (Wu et al., 2020), while a calcium-chelating peptide isolated from Pacific cod skin gelatin showed the ability to improve calcium absorption (Wu et al., 2017). In addition, active peptides derived from pacific cod skin demonstrated antioxidant activity and angiotensin-I converting enzyme inhibitory ability (Ngo et al., 2011). Moreover, further research that clarified the underlying mechanism was mediated by regulation of the MAPK and transforming growth factor-β/Smad signaling pathways (Chen and Hou, 2016; Chen et al., 2016). However, there is little information about the protective effect of *Melanogrammus aeglefinus* skin oligopeptide (MSOP) in UVB-irradiated human keratinocytes, and the underlying mechanism remains unclear.

In this study, the method of preparing MSOP was optimized, the composition and abundance of peptides in MSOP was identified by MALDI-TOF/TOF, the function of peptides was predicted by Discovery Studio 2019, the protective effect of MSOP was explored in UVB-irradiated human keratinocytes, and the underlying mechanism was investigated by proteomics. We proposed that MSOP has potential applications in UVB-induced photoaging.

2. Materials and methods

2.1. Optimizing the method used to prepare MSOP

Pepsin (Shanghai Yuanye Bioengineering Institute, Shanghai, China) was selected to hydrolyze *Melanogrammus aeglefinus* skin collagen (Shanghai Nitta Gelatin Co., Ltd, Shanghai, China) according to previous studies (Song et al., 2022). Single-factor experiments were performed to establish the range of independent variables [temperature, enzyme/substrate (E/S) ratio and time]. Then Box-Behnken response surface design was formulated to evaluate and optimize the effects of these three independent variables and their interactions on the degree of hydrolysis (DH). The DH was measured by trichloroacetic acid soluble nitrogen method as previously described (Rutherfurd, 2010), and calculated by following formula: DH (%) = [content of amino nitrogen in supernatant (mg/ml)/total content of nitrogen in sample (mg/mL)] × 100%.

2.2. Peptide sequence identification

The peptide composition in MSOP was measured by MALDI-TOF/TOF 5800 (AB Sciex, Framingham, MA, USA) at Jiyun Biotechnology Co., Ltd. (Shanghai, China) as previously described (Lu et al., 2021). MS spectra were collected in a molecular mass range of 500–3,000 Da, the peak detection signal-to-noise ratio was set to 15, and MS/MS spectra were analyzed to identify peptides using the Mascot Server (Matrix Science Inc, Boston, MA, USA) with the NCBI nr database.

2.3. Molecular docking with Discovery Studio 2019

The molecular structures of peptides were built, and energy was minimized using Discovery Studio 2019. The X-ray structure of Keap1 (PDB ID: 5DAD) was retrieved from the Protein Data Bank (https://www.rcsb.org), the water molecules, native ligands and heteroatom molecules were removed by Discovery Studio 2019, and PyRx 0.9 software was used to minimize the energy of the protein. Then, the CDOCKER module in Discovery Studio 2019 was selected for molecular docking using the default settings as previously described (Fan et al., 2022).

2.4. Cell culture and UVB irradiation

The HaCaT cell line was purchased from Beyotime Biotechnology (Shanghai, China), and cultured in Dulbecco's modified Eagle's medium (DMEM) (Hyclone, Logan, UT, USA) supplemented with 10% fetal bovine serum (FBS) (Hyclone) and 1% antibiotics (Hyclone) at 37 °C and 5% CO_2 in a humidified incubator. HaCaT cells were seeded and adhered for 24 h. The cells were treated with various concentrations of MSOP and subsequently exposed to UVB radiation at a dose of 50 mJ/cm^2 according to previous studies (Xiao et al., 2021). Cells without MSOP or UVB irradiation treatments were served as the control.

2.5. Cell viability assay

HaCaT cells (1×10^5) were seeded in 96-well culture plates and treated with various concentrations of MSOP for 24 h. Then, an MTT assay kit purchased from Nanjing Jiancheng Bioengineering Institute (Nanjing, Jiangsu, China) was used to measure the cell proliferation and cytotoxicity in response to MSOP treatments at different concentrations.

2.6. Antioxidant enzyme activities

MDA, SOD and GSH-Px activities were measured using colorimetric assay kits (Nanjing Jiancheng Bioengineering Institute) according to the manufacturer's protocol.

2.7. Apoptosis detection

Cells were washed with PBS, stained with an Annexin V-FITC/PI kit (Beyotime Biotechnology), and measured with a CytoFLEX Flow Cytometer (Beckman Coulter, Inc. Brea, CA, USA). In addition, the apoptotic rate was analyzed by Modfit LT 6.0 software (www.vsh.com).

2.8. Quantitative proteomic analysis

According to the previous method (Miles et al., 2023), the cell pellet was extracted with lysis buffer. The protein extract was centrifuged at 15,000 g at 4 °C for 20 min, the supernatant was treated with acetone to precipitate protein, and NH_4HCO_3 solution (40 mM) was added to the pellets. The protein concentration was measured by a BCA protein assay kit (Nanjing Jiancheng Bioengineering Institute). Then, the proteins were reduced and alkylated before digestion by trypsin (Promega Corporation, Madison, WI, USA). The digestion was stopped by formic acid, and the samples were then vacuum-dried.

Digested peptides were separated with chromatography by an Easy-nLC1000 system (Thermo Fisher Scientific, Am Kalkberg, Osterode, Germany) as previously described (J. Guo et al., 2017). Separated peptides were detected in the Orbitrap Fusion mass

Table 1. The potential targets of three peptides with high fit value screened by Discovery Studio 2019

Peptide	Pharmacophore	Fit value	Biological function
VADML	4zy3-04: Kelch-like ECH-associated protein 1	3.9737	Antioxidation
	1pg4-06: Acetyl-coenzyme A synthetase	3.8309	Biosynthesis of antibiotics
	1uk4-02: Replicase polyprotein 1ab	3.81262	Severe acute respiratory syndrome
IARF	5dad-08: Kelch-like ECH-associated protein 1	3.78306	Antioxidation
	1a4h-07: ATP-dependent molecular chaperone HSP82	3.73784	cancer
SSPSF	1tyr-01: Transthyretin	3.92604	Hyperthyroxinemia,
	1tqf-02: Beta-secretase 1	3.91493	Alzheimer's disease
	4zy3-03: Kelch-like ECH-associated protein 1	3.85125	Antioxidation
	1m48-04: Interleukin-2	3.77783	Type I diabetes mellitus
	3cqw-09: RAC-alpha serine/threonine-protein kinase	3.75172	cancer

spectrometer (Thermo Fisher Scientific) with a Michrom captive spray nanoelectrospray ionization (NSI) source. Spectra were scanned over the m/z range 300–4,000 Da at 120,000 resolution.

The raw data were further examined by PEAKS software (version 7.5, Bioinformatics Solutions, Waterloo, Canada) as previously described and a label-free approach was performed to detect the relative quantification by the Q module in PEAKS (Yang et al., 2023). Proteins were considered to be significant when $p < 0.05$ and a fold change of ≥2.

Bioinformatics analysis was performed according to a previous method (J. Liu et al., 2015). Functional annotation was performed by Blast2GO, (version 6.0.1) and protein pathway analysis was performed by the Kyoto Encyclopedia of Genes and Genomes (http://www.genome.jp/kegg).

2.9. Quantitative real-time PCR (qRT-PCR) analysis

As previously described (Huang et al., 2021), total RNA was isolated and purified by the TransZol Up Plus RNA kit (Beijing TransGen Biotech Co., Ltd., Beijing, China), cDNA was reverse transcribed by TransScript® All-in-One First-Strand cDNA Synthesis SuperMix for qPCR (Beijing TransGen Biotech Co., Ltd), and the primers used in this study are presented in Table S1. The mRNA level of the target gene was calculated by the $2^{-\Delta\Delta CT}$ method and normalized to the β-actin level.

2.10. Statistical analysis

All data are presented as the mean ± standard deviation (SD). The normally distributed data were assessed by ANOVA followed by Tukey's post hoc test (SPSS, version 19.0, Chicago, IL, USA), and data that did not meet the assumptions of ANOVA were analyzed by the Mann-Whitney test (MATLAB R2012a, Natick, MA, USA). Statistical significance was defined as $p < 0.05$.

3. Results

3.1. Optimization of MSOP preparation

In single-factor experiments, the results showed that the optimum hydrolysis conditions of time, temperature and E/S ratio were 3.5–4.5 h, 25–35 °C and 0.5–1.5%, respectively (Figure S1a–c). In addition, the response surface experiment showed that DH (%) = $87.75 - 0.58A - 1.31B + 0.080C + 0.020AB + 0.33AC + 0.55BC - 6.52A^2 - 5.41B^2 - 5.01C^2$ (Where A is the time; B the temperature; C the amount of enzyme), and the most suitable variables for the time, temperature and E/S ratio were 4.31 h, 32.30 °C and 1.25%, respectively. (Figure S1d and Table S2–3). At that optimized condition, the DH reached 83.71%, while the predicted DH was 80.24%.

3.2. Composition of MSOP

The compositions of peptides in MSOP were determined by MALDI-TOF/TOF. The results of the first-order mass spectrometry showed that the majority of the parent ions were less than m/z 1,000 (Figure S2a). Three peptides were found to be dominant in the MSOP, with molecular weights of 506.2860 Da, 524.2478 Da and 524.2478 Da, respectively (Figure S2b–d). Further analysis by second-order mass spectrometry identified the amino acid sequences of these three peptides, which were VADML (Val-Ala-Asp-Met-Leu), IARF (Ile-Ala-Arg-Phe) and SSPSF (Ser-Ser-Pro-Ser-Phe)

3.3. Predicted interactions between three peptides and Keap1

In this study, a total of 44 target pharmacophores were predicted to interact with three peptides. We compared the fit value of peptides with those of targets, and the targets with high fit values are listed in Table 1. The results showed that VADML, IARF and SSPSF interacted with Keap1 (4zy3 and 5dad), playing a vital role in the Keap1/Nrf2-ARE pathway involved in oxidative stress regulation. Therefore, Keap1 was used as the receptor for subsequent molecular docking.

The interactions between the peptides and Keap1 were characterized with E_{CI}, E_{VDW} and RMS Gradient. As shown in Table 2, the $-E_{CI}$ values of VADML, IARF and SSPSF were 92.3, 73.6 and 63.0, respectively, while the corresponding $-E_{VDW}$ values were 10.1, 5.6 and 3.7. According to Figure 1a, there are seven amino acid residues of Keap1 that interact with VADML. Among them, $Arg^{B:233}$ formed attractive charges, $Ser^{B:231}$ and $Gln^{B:276}$ formed conventional hydrogen bonds, $Trp^{B:232}$, $Ser^{B:239}$ and $Pro^{B:235}$ formed carbon hydrogen bonds, and $Tyr^{B:230}$ formed pi-alkyl groups. There are nine amino acid residues involved in the interac-

Table 2. The molecular docking results of three peptides with Keap1

Peptide	Amino Acid Sequence	-E_{CI} (kJ/mol)	-E_{VDW} (kJ/mol)	RMS Gradient
VADML	Val-Ala-Asp-Met-Leu	92.2685	10.0515	0.00935
IARF	Ile-Ala-Arg-Phe	73.5967	5.61457	0.00984
SSPSF	Ser-Ser-Pro-Ser-Phe	63.0232	3.69658	0.00985

tions between IARF and Keap1 (Figure 1b). Among them, $Asp^{B:278}$ and $Asp^{B:279}$ formed attractive charges, $Ser^{B:231}$, $Arg^{B:233}$, $Trp^{B:240}$, $Ser^{B:275}$ and $Gln^{B:276}$ formed conventional hydrogen bonds, and $Pro^{B:235}$ and $Ser^{B:275}$ produced carbon hydrogen bonds. There are 7 seven amino acid residues involved in SSPSF interactions with Keap1 (Figure 1c). $Gln^{B:276}$, $Ser^{B:231}$, $Ser^{B:234}$ and $Trp^{B:240}$ formed conventional hydrogen bonds, TrpB:232 formed carbon hydrogen bonds and $Trp^{B:230}$ and $Phe^{B:282}$ formed pi-alkyl bonds.

3.4. Protective effects of MSOP against UVB-induced injury in HaCaT cells

We investigated the effect of MSOP on the proliferation of HaCaT cells after exposure to UVB. Cell viability was reduced to 57.37% by UVB irradiation in the absence of MSOP but significantly restored with MSOP treatment, and the highest cellular survival rate was observed in the high dosage MSOP-treated group (Figure 2a).

3.5. Antioxidant effects of MSOP in UVB-induced HaCaT cells

To investigate whether the radical scavenging activity of MSOP was mediated by antioxidant enzymes, the activities of antioxidant enzymes were examined in HaCaT cells after UVB exposure. SOD and GSH-Px activity were enhanced by MSOP treatments in a dose-dependent manner. Furthermore, in comparison with the control group, the level of MDA in the UVB-induced group was increased, but treatment with MSOP decreased the level of MDA (Figure 2b–d).

3.6. Protective effects of MSOP against UVB-induced apoptosis

The lower left quadrant represents viable and healthy cells, which were decreased by UVB treatment, but restored after MSOP treatment at a high dosage. The right quadrant represents the apoptotic cells, including early and late apoptotic cells, which decreased from 21.3% to 16.2% in MSOP-treated cells (Figure 3).

3.7. Analysis of differentially expressed proteins

Figure 4a shows the overlap of differentially expressed proteins (DEPs) (fold change ≥2 or ≤0.5) from the control, LD, MD and HD groups compared to the UVB group. The numbers of DEPs in the control, LD, MD, and HD groups were 286, 204, 176 and 157, respectively. Among them, 119 proteins were upregulated and 167 were downregulated. The numbers of DEPs upregulated in LD, MD, and HD were 98, 104, and 79, respectively, while the corresponding numbers for downregulation were 106, 72 and 78. In addition, 23 DEPs were identified in all pairwise comparisons (Figure 4b and Table S4).

To validate the accuracy of the proteomic data, the mRNA levels of 12 DEPs were assessed by qRT-PCR. Figure 5 shows that seven DEPs (*qcr2*, *calX*, *uba1*, *dhe3*, *lap2B*, *ehd2* and *nrf2*) were upregulated, and the remaining five DEPs (*6 pgd*, *serA*, *keaP1*, *lamP1* and *ero1A*) were downregulated. The Pearson correlation coefficients for proteomics and qRT-PCR data were ≥ 0.9.

3.8. Functional analysis of DEPs

The proteins with increased expression were categorized as biological processes (BP), cellular components (CC), or molecular functions (MF). In the comparison of UVB and HD, the proteins with increased expression in the BP category were posttranscriptional gene silencing by RNA, regulation of apoptosis involved in tissue homeostasis, reactive nitrogen species metabolic process, etc. The proteins in the CC category were RISC complex, dense body and peroxisomal matrix. The proteins in the MF category were RNA polymerase III regulatory region DNA binding, peroxynitrite reductase activity, transcription cofactor activity, etc (Figure 4c). The proteins with decreased expression in the BP category were defense response to sensory perception of sound, exocytosis, cellular response to osmotic stress, etc. The proteins in the CC category were proteasome activator complex and exocyst, while the proteins in the MF category were SNARE binding, protease binding, serine-type endopeptidase inhibitor activity, etc (Figure 4d). In addition, the results from KEGG differential pathway analysis showed that the DEPs were involved in 9 metabolic pathways that were mainly related to the oxidative stress pathway (Table S5).

4. Discussion

Biologically active peptides are inactive within the sequence of their parent protein and can be released by enzymatic hydrolysis either during gastrointestinal digestion or food processing (Dhar et al., 2023; Ucak et al., 2021). In this study, MSOP was prepared via pepsin, the major components were identified to be VADML, IARF and SSPSF, and the potential antioxidant activity was predicted by Discovery Studio 2019. In addition, a UVB-induced HaCaT cell model was established to explore the anti-photoaging and antioxidant activity of MSOP *in vitro*, and this cell model was widely used in evaluating the anti-photoaging activity of *Salvia plebeia* R. Br ethanol extract, bioactive peptides from *Skipjack Tuna* cardiac arterial bulbs and flexible liposomes co-loaded with apigenin and doxycycline as previously described (Guo et al., 2023; Kong et al., 2023; Liu et al., 2023)

Discovery Studio is a powerful research platform for the life sciences that integrates a comprehensive suite of informatics, modeling and simulation solutions (Han et al., 2020). From the results of reverse docking, we found that all three peptides interacted with Keap1 (4zy3 and 5dad) (Table 1). Nuclear factor erythroid 2-like 2 (Nrf2), is a transcription factor that serves as a key regulator of the cellular response to oxidative stress. Under normal physiological conditions, Keap1 maintains low levels of Nrf2 by promoting its Cul3-rbx1-mediated ubiquitination and subsequent proteasomal degradation. Under stressful conditions, ROS modify sensor

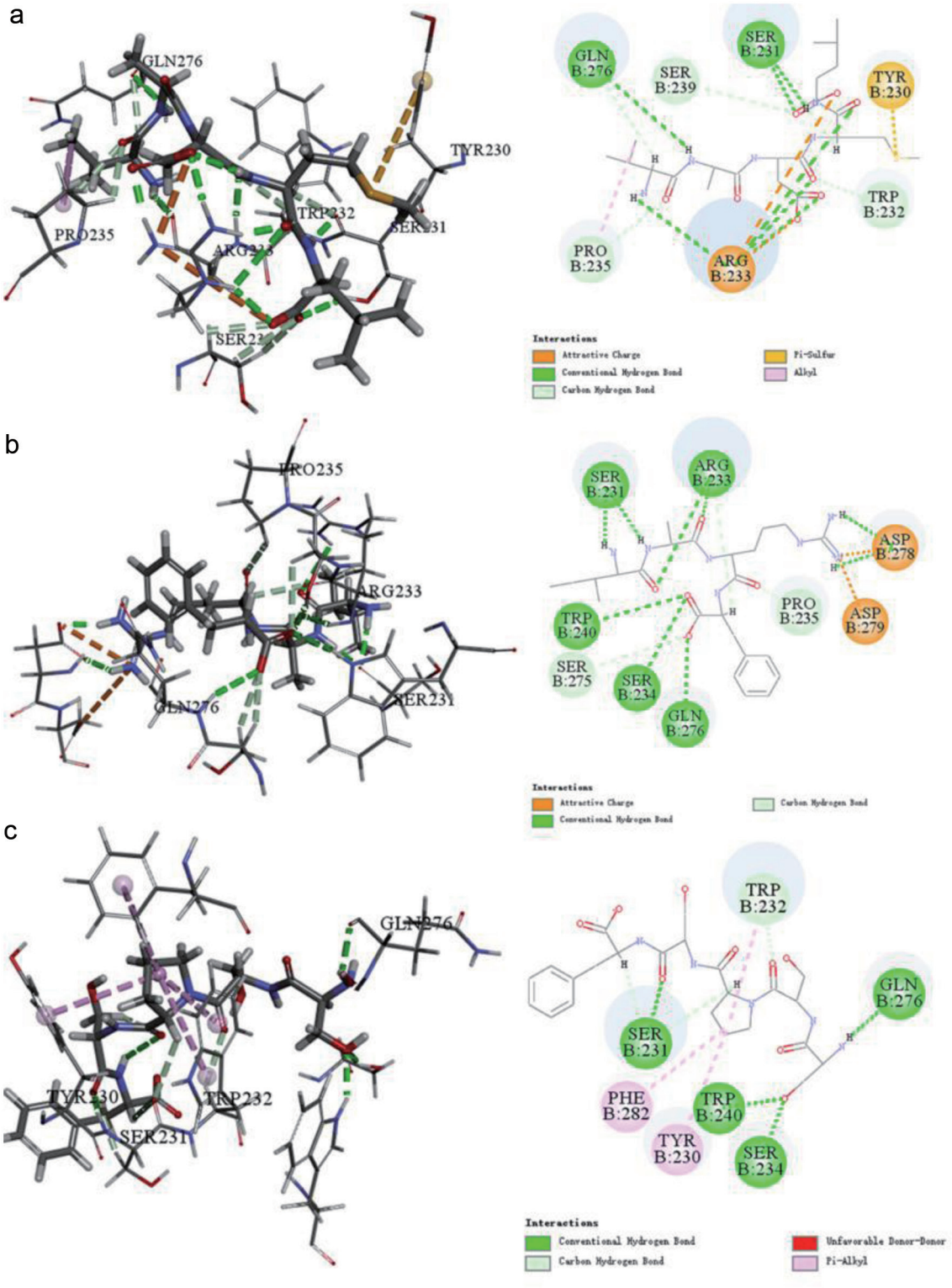

Figure 1. Interactions between Keap1 and peptide predicated Discovery Studio 2019. (a) VADML, (b) IARF, (c) SSPSF.

cysteine residues within Keap1 and block the degradation of Nrf2. Newly synthesized Nrf2 then translocates to the nucleus, binds to antioxidant response elements, and increases the transcription of numerous genes that encode cellular defense and repair enzymes (Ong et al., 2023; Suzuki et al., 2023). This coordinated and rapid upregulation of multiple genes ensures a robust response to many

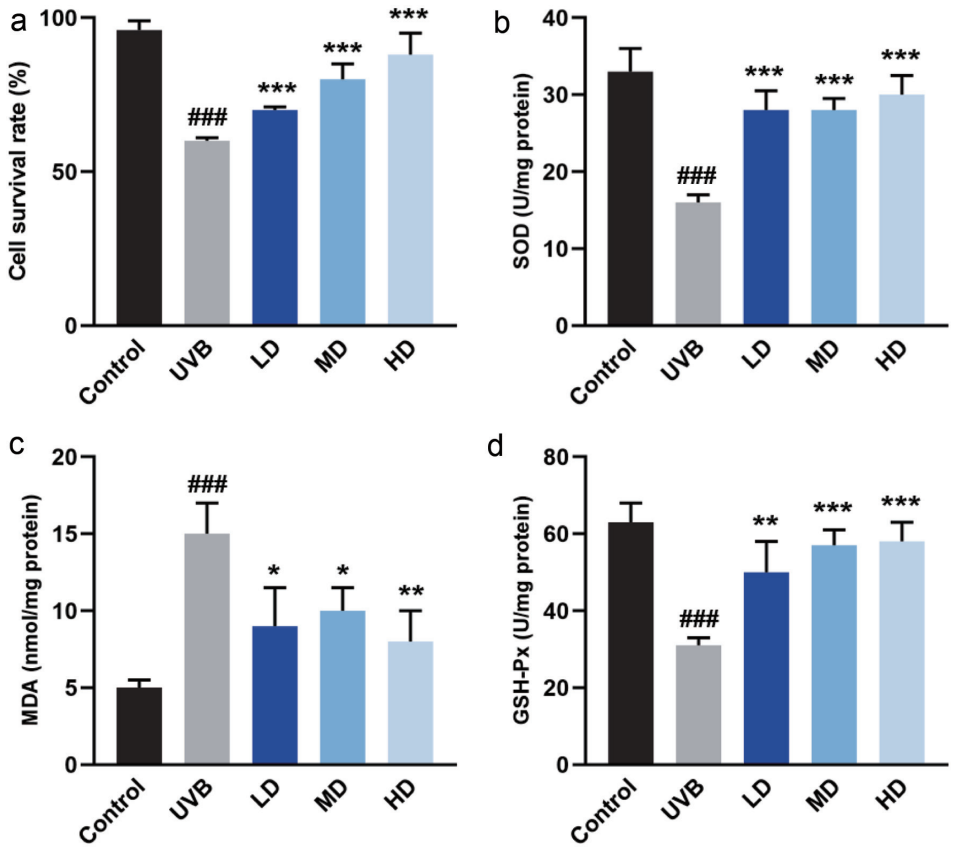

Figure 2. Antioxidant activity of MSOP in human keratinocytes HaCaT cells exposed to UVB. (a) Cell viability in response to UVB and MSOP treatments. (b) activity of SOD. (c) Content of MDA. (d) Activity of GSH-Px. ### $p < 0.001$ compared to control group. *$p < 0.05$, **$p < 0.01$ and ***$p < 0.001$ compared to UVB group.

types of cellular stress (Dai et al., 2023). The results of molecular docking showed that VADML, IARF and SSPSF interacted with Keap1 and showed potential Keap1 inhibitory activity (Figure 1). Thus, we proposed a tentative inference that MSOP played an antioxidative role by regulating the Keap1-Nrf2/ARE signaling pathway.

Superoxide radicals are formed in all living cells exposed to oxygen, by various biochemical systems in the cells. SOD catalyzes dismutation of the superoxide anion (O^{2-}) into hydrogen peroxide, which protects organisms against the toxic effects of superoxide radicals (Khayatan et al., 2023). GSH-Px is located primarily in the cytosol and has a general specificity in detoxifying H_2O_2 and converting lipid hydroperoxides to nontoxic alcohols (Brigelius-Flohé and Flohé, 2020). MDA can exacerbate the actions of superoxide ions by impairing endothelium dependent relaxation and propagation of lipid peroxidation by chain reaction in membranes (Del Rio et al., 2005). In our experiment, MSOP treatment dose-dependently increased the activities of SOD and GSH-Px, and decreased the content of MDA (Figure 2), which activated the defensive mechanism against ROS attack in the living HaCaT cells.

However, the underlying mechanism mechanism of MSOP activity in the UVB-irradiated HaCaT cellular model is extremely complex, and it remains unclear which proteins are involved in the beneficial effects of MSOP. Therefore, quantitative proteome

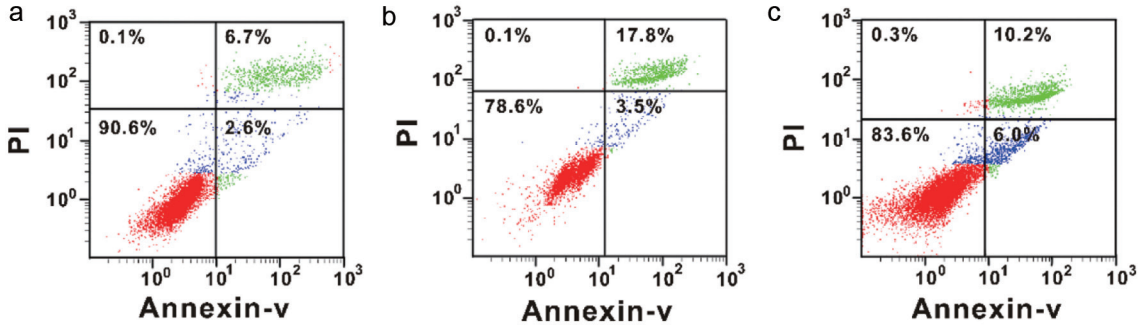

Figure 3. The anti-apoptosis effects of MSOP measured by flow cytometric analysis. (a) Control group. (b) UVB group. (d) High-dosage UVB group.

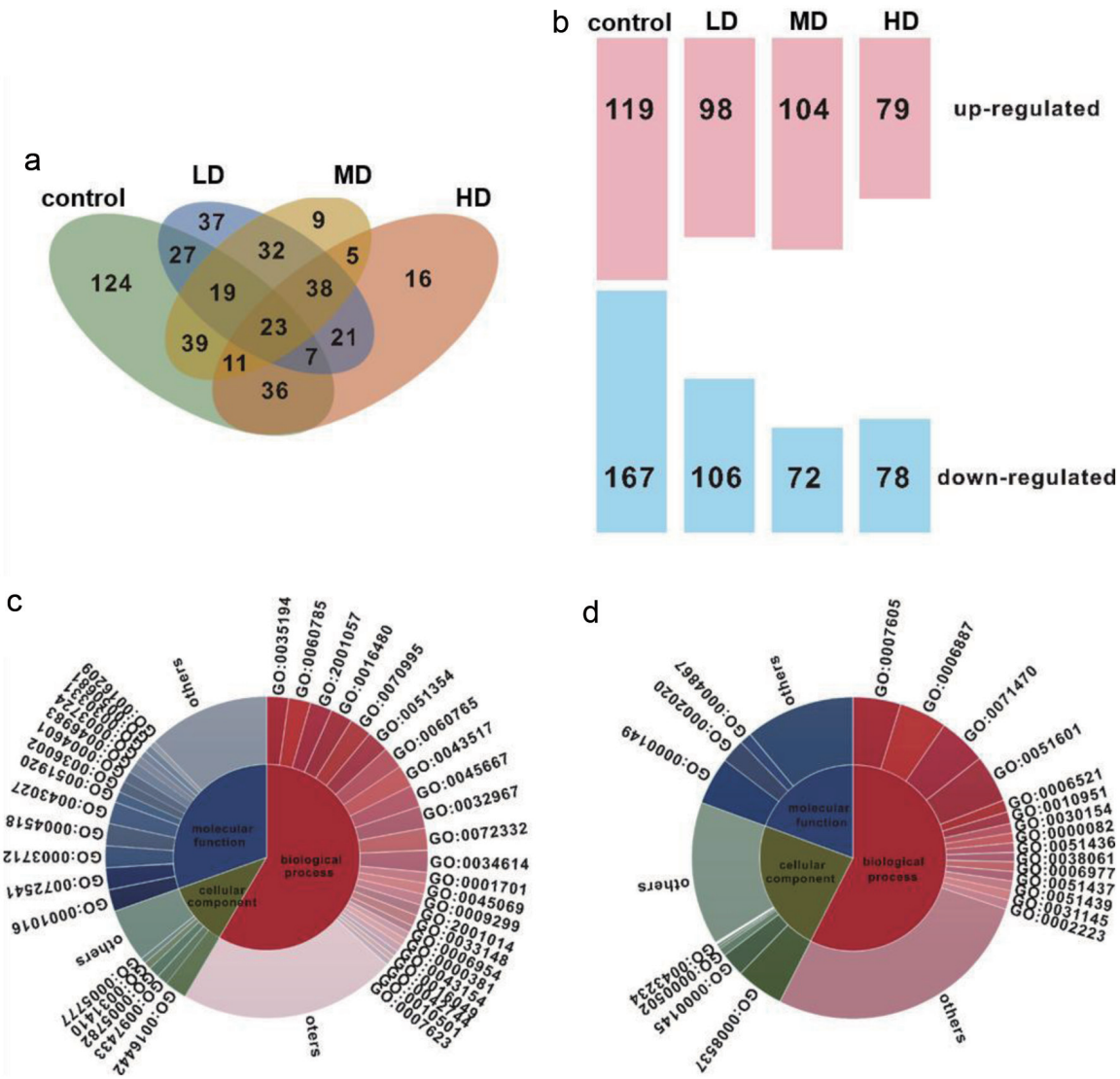

Figure 4. Quantitative proteome analysis in HaCaT cells in response to UVB and MSOP treatments. (a) Venn diagram of differentially expressed proteins (DEPs) (fold change ≥2 or ≤0.5) in response to UVB and MSOP treatments. (b) Numbers of upregulated and downregulated proteins in HaCaT cells. Upregulated (c) and downregulated (d) DEPs categorized by biological process, molecular function, and cellular component.

technology was used in this study. Research has shown that that the Keap1/Nrf2/ARE signaling pathway plays a significant role in protecting cells from oxidative stress (Hassanein et al., 2020; Shi et al., 2021; Yuan et al., 2020). Under quiescent conditions, the transcription factor Nrf2 interacts with the actin-anchored protein Keap1, which is largely localized in the cytoplasm. This quenching interaction maintains low basal expression of Nrf2-regulated genes. However, upon UVB- irradiated photodamage, Nrf2 is released from Keap1, escapes proteasomal degradation, translocates to the nucleus, and transactivates the expression of several dozen cytoprotective genes that enhance cell survival (Figure 6). The present study showed that the MSOP caused significant upregulation of Nrf2 and downregulation of Keap1 in HaCaT cells, which may contribute to the beneficial effects of MSOP in a UVB-induced HaCaT cellular model.

In conclusion, we optimized the preparation method of MSOP with an 80.24% degree of hydrolysis and identified three peptides (VADML, IARF and SSPSF), which were highly abundant and predicted to show potential antioxidant activity due to their interactions with Keap1 via Discovery Studio 2019 simulation. In addition, the antioxidant activity of MSOP was investigated in vitro via a UVB-induced HaCaT cell injury model, and the underlying mechanism was explored via quantitative proteomics, especially on the regarding of the Keap1/Nrf2/ARE pathway. MSOP might offer an alternative for protecting skin against UVB exposure.

Acknowledgments

This work was sponsored by Regional Demonstration Project of Marine Economic Innovation and Development in 2014 and 2016, the National Key Research and Development Program of China (2018YFD0901102), and K.C. Wong Magna Fund of Ningbo University.

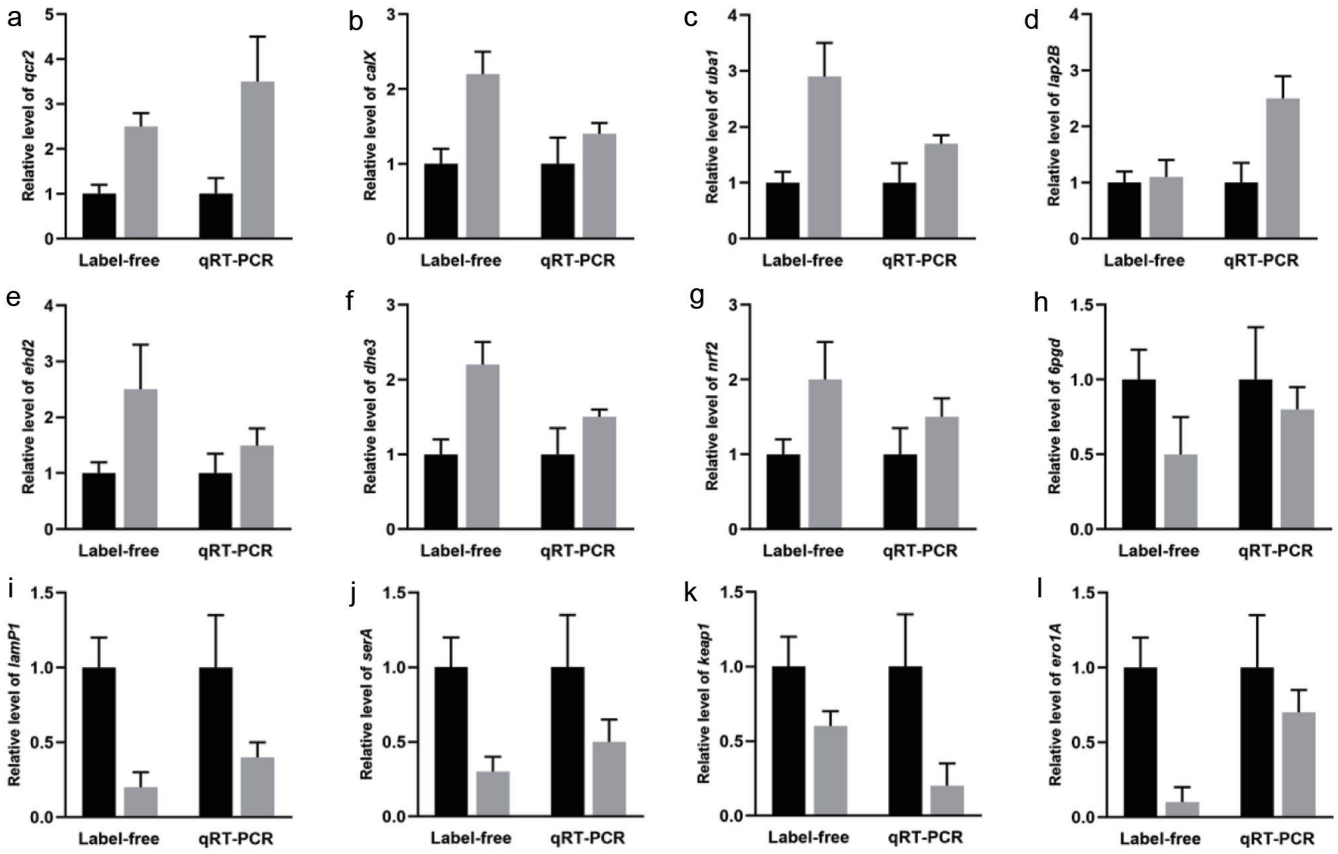

Figure 5. Expression of differentially expressed proteins measured by quantitative proteome and qRT-PCR in HaCaT cells. (a) *qcr2*, (b) *calX*, (c) *uba1*, (d) *dhe3*, (e) *lap2B*, (f) *ehd2*, (g) *nrf2*, (g) *6pgd*, (i) *serA*, (j) *keap1*, (k) *lamP1*, (l) *ero1A*.

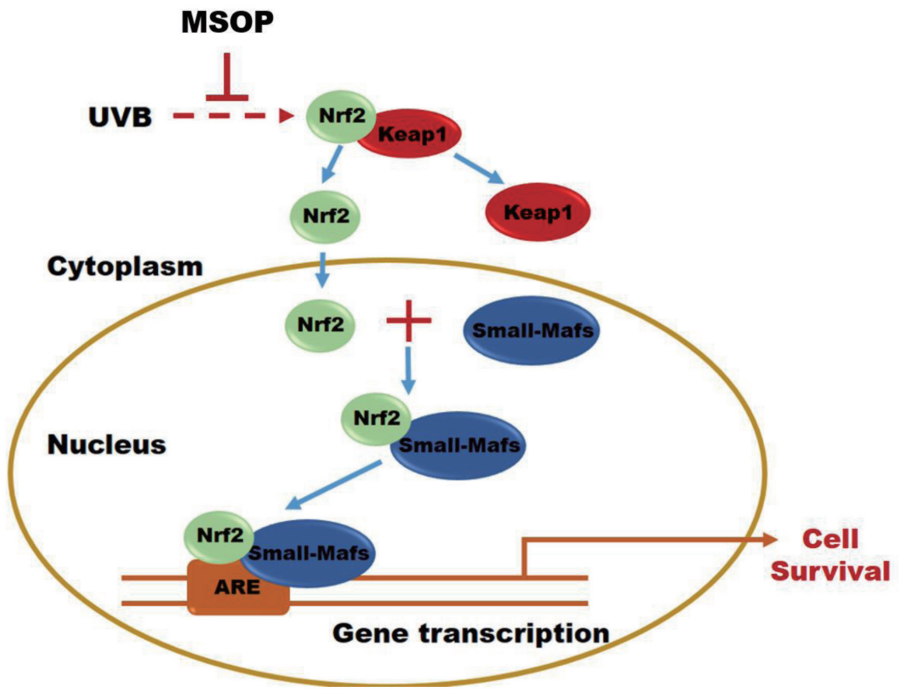

Figure 6. General scheme for the beneficial effects of MSOP through Keap1/Nrf2/ARE signaling pathway regulation.

Conflict of interest

The authors report no conflict of interest.

Supplementary material

Table S1. Primers used in this study for qRT-PCR.

Table S2. Central composite design quadratic polynomial model, experimental data and actual values.

Table S3. ANOVA for the quadratic polynomial model.

Table S4. Twenty-three DEPs were identified in all comparisons with the UVB group.

Table S5. KEGG pathway analysis of DEPs.

Figure S1. Optimization of enzymatic hydrolysis conditions. Effect of time (a), temperature (b) and E/S ratio (c) on the enzymatic treatment. (d) 3D and 2D response surfaces demonstrating the effects of enzymolysis conditions.

Figure S2. Identification of the molecular mass and amino acid sequence of the peptides from MSOP. (a) Full MS scan. MS/MS spectrum of the ion 506.2860 m/z (b), 524.2478 m/z (c) and 548.1384 m/z (d).

Figure S3. Cell survival rate of HaCaT cells at different concentrations of MSOP.

References

Berry, K., Hallock, K., and Lam, C. (2022). Photoaging and topical rejuvenation. Facial. Plast. Surg. Clin. North Am. 30(3): 291–300.

Brigelius-Flohé, R., and Flohé, L. (2020). Regulatory phenomena in the glutathione peroxidase superfamily. Antioxid. Redox. Signal. 33(7): 498–516.

Bruno Siewe, F., Kudre, T.G., and Narayan, B. (2021). Optimisation of ultrasound-assisted enzymatic extraction conditions of umami compounds from fish by-products using the combination of fractional factorial design and central composite design. Food Chem. 334: 127498.

Chen, K., Yang, Q., Hong, H., Feng, L., Liu, J., and Luo, Y. (2020). Physicochemical and functional properties of Maillard reaction products derived from cod (Gadus morhua L.) skin collagen peptides and xylose. Food Chem. 333: 127489.

Chen, T., and Hou, H. (2016). Protective effect of gelatin polypeptides from Pacific cod (Gadus macrocephalus) against UV irradiation-induced damages by inhibiting inflammation and improving transforming growth factor-β/Smad signaling pathway. J. Photochem. Photobiol. B 162: 633–640.

Chen, T., Hou, H., Fan, Y., Wang, S., Chen, Q., Si, L., and Li, B. (2016). Protective effect of gelatin peptides from pacific cod skin against photoaging by inhibiting the expression of MMPs via MAPK signaling pathway. J. Photochem. Photobiol. B 165: 34–41.

Dai, X., Zhang, Q., Zhang, G., Ma, C., and Zhang, R. (2023). Protective effect of agar oligosaccharide on male Drosophila melanogaster suffering from oxidative stress via intestinal microflora activating the Keap1-Nrf2 signaling pathway. Carbohydr. Polym. 313: 120878.

Del Rio, D., Stewart, A.J., and Pellegrini, N. (2005). A review of recent studies on malondialdehyde as toxic molecule and biological marker of oxidative stress. Nutr. Metab. Cardiovasc. Dis. 15(4): 316–328.

Dhar, H., Verma, S., Dogra, S., Katoch, S., Vij, R., Singh, G., and Sharma, M. (2023). Functional attributes of bioactive peptides of bovine milk origin and application of in silico approaches for peptide prediction and functional annotations. Crit. Rev. Food Sci. Nutr. 1–23.

Fan, S., Huang, Y., Lu, G., Sun, N., Wang, R., Lu, C., Ding, L., Han, J., Zhou, J., Li, Y., Ming, T., and Su, X. (2022). Novel anti-hyperuricemic hexapeptides derived from *Apostichopus japonicus* hydrolysate and their modulation effects on the gut microbiota and host microRNA profile. Food Funct. 13(7): 3865–3878.

Fernandes, A., Rodrigues, P.M., Pintado, M., and Tavaria, F.K. (2023). A systematic review of natural products for skin applications: Targeting inflammation, wound healing, and photo-aging. Phytomedicine 115: 154824.

Freitas-Rodríguez, S., Folgueras, A.R., and López-Otín, C. (2017). The role of matrix metalloproteinases in aging: Tissue remodeling and beyond. Biochim. Biophys. Acta. Mol. Cell Res. 1864(11 Pt A): 2015–2025.

Guo, J., Wang, P., Cheng, Q., Sun, L., Wang, H., Wang, Y., Kao, L., Li, Y., Qiu, T., Yang, W., and Shen, H. (2017). Proteomic analysis reveals strong mitochondrial involvement in cytoplasmic male sterility of pepper (Capsicum annuum L.). J. Proteomics. 168: 15–27.

Guo, Y., Zhang, Y., Wang, Y.S., Ma, L., Liu, H., and Gao, W. (2023). Protective effect of *Salvia plebeia* R. Br ethanol extract on UVB-induced skin photoaging *in vitro* and *in vivo*. Photodermatol. Photoimmunol. Photomed.

Han, J., Huang, Z., Tang, S., Lu, C., Wan, H., Zhou, J., Li, Y., Ming, T., Jim Wang, Z., and Su, X. (2020). The novel peptides ICRD and LCGEC screened from tuna roe show antioxidative activity via Keap1/Nrf2-ARE pathway regulation and gut microbiota modulation. Food Chem. 327: 127094.

Hassanein, E.H.M., Sayed, A.M., Hussein, O.E., and Mahmoud, A.M. (2020). Coumarins as modulators of the Keap1/Nrf2/ARE signaling pathway. Oxid. Med. Cell Longev. 2020: 1675957.

Hooda, R., Madke, B., and Choudhary, A. (2023). Photoaging: reversal of the oxidative atress through dietary changes and plant-based products. Cureus 15(4): e37321.

Huang, Y., Fan, S., Lu, G., Sun, N., Wang, R., Lu, C., Han, J., Zhou, J., Li, Y., Ming, T., and Su, X. (2021). Systematic investigation of the amino acid profiles that are correlated with xanthine oxidase inhibitory activity: Effects, mechanism and applications in protein source screening. Free Radic. Biol. Med. 177: 326–336.

Khayatan, D., Razavi, S.M., Arab, Z.N., Hosseini, Y., Niknejad, A., Momtaz, S., Abdolghaffari, A.H., Sathyapalan, T., Jamialahmadi, T., Kesharwani, P., and Sahebkar, A. (2023). Superoxide dismutase: a key target for the neuroprotective effects of curcumin. Mol. Cell Biochem.

Kong, J., Hu, X.M., Cai, W.W., Wang, Y.M., Chi, C.F., and Wang, B. (2023). Bioactive peptides from *Skipjack Tuna* cardiac arterial bulbs (II): protective function on UVB-irradiated HaCaT cells through antioxidant and anti-apoptotic mechanisms. Mar. Drugs 21(2): .

Kumar, K.J.S., Vani, M.G., and Wang, S.Y. (2022). Limonene protects human skin keratinocytes against UVB-induced photodamage and photoaging by activating the Nrf2-dependent antioxidant defense system. Environ. Toxicol. 37(12): 2897–2909.

Löwenau, L.J., Zoschke, C., Brodwolf, R., Volz, P., Hausmann, C., Wattanapitayakul, S., Boreham, A., Alexiev, U., and Schäfer-Korting, M. (2017). Increased permeability of reconstructed human epidermis from UVB-irradiated keratinocytes. Eur. J. Pharm. Biopharm. 116: 149–154.

Lim, H.S., Simon, S.E., Yow, Y.Y., Saidur, R., and Tan, K.O. (2022). Photoprotective activities of *Lignosus rhinocerus* in UV-irradiated human keratinocytes. J. Ethnopharmacol. 299: 115621.

Liu, C., Guo, X., Chen, Y., Zhao, M., Shi, S., Luo, Z., Song, J., Zhang, Z., Yang, W., and Liu, K. (2023). Anti-photoaging effect and mechanism of flexible liposomes co-loaded with apigenin and doxycycline. Biomed. Pharmacother. 164: 114998.

Liu, H.M., Tang, W., Wang, X.Y., Jiang, J.J., Zhang, W., and Wang, W. (2023). Safe and effective antioxidant: the biological mechanism and potential pathways of ergothioneine in the skin. Molecules 28(4): .

Liu, J., Pang, C., Wei, H., Song, M., Meng, Y., Ma, J., Fan, S., and Yu, S. (2015). iTRAQ-facilitated proteomic profiling of anthers from a photosensitive male sterile mutant and wild-type cotton (*Gossypium hirsutum* L.). J. Proteomics. 126: 68–81.

Lu, C., Tang, S., Han, J., Fan, S., Huang, Y., Zhang, Z., Zhou, J., Ming, T., Li, Y., and Su, X. (2021). *Apostichopus japonicus* oligopeptide induced heterogeneity in the gastrointestinal tract microbiota and alleviated

hyperuricemia in a microbiota-dependent manner. Mol. Nutr. Food Res. 65(14): e2100147.

Masaki, H., Izutsu, Y., Yahagi, S., and Okano, Y. (2009). Reactive oxygen species in HaCaT keratinocytes after UVB irradiation are triggered by intracellular Ca(2+) levels. J. Investig. Dermatol. Symp. Proc. 14(1): 50–52.

Miles, H.N., Tomlin, D., Ricke, W.A., and Li, L. (2023). Integrating intracellular and extracellular proteomic profiling for in-depth investigations of cellular communication in a model of prostate cancer. Proteomics .

Ngo, D.H., Ryu, B., Vo, T.S., Himaya, S.W., Wijesekara, I., and Kim, S.K. (2011). Free radical scavenging and angiotensin-I converting enzyme inhibitory peptides from Pacific cod (Gadus macrocephalus) skin gelatin. Int. J. Biol. Macromol. 49(5): 1110–1116.

Oh, J.H., Lee, J.I., Karadeniz, F., Park, S.Y., Seo, Y., and Kong, C.S. (2020). Antiphotoaging effects of 3,5-Dicaffeoyl-epi-quinic acid via inhibition of matrix metalloproteinases in UVB-irradiated human keratinocytes. Evid. Based Complement Alternat. Med. 2020: 8949272.

Ong, A.J.S., Bladen, C.E., Tigani, T.A., Karamalakis, A.P., Evason, K.J., Brown, K.K., and Cox, A.G. (2023). The KEAP1-NRF2 pathway regulates TFEB/TFE3-dependent lysosomal biogenesis. Proc. Natl. Acad. Sci. U S A 120(22): e2217425120.

Rutherfurd, S.M. (2010). Methodology for determining degree of hydrolysis of proteins in Hydrolysates: a review. J. AOAC Int. 93(5): 1515–1522.

Shi, X., Cheng, W., Wang, Q., Zhang, J., Wang, C., Li, M., Zhao, D., Wang, D., and An, Q. (2021). Exploring the protective and reparative mechanisms of *G. lucidum* polysaccharides against H_2O_2-induced oxidative stress in human skin fibroblasts. Clin. Cosmet. Investig. Dermatol. 14: 1481–1496.

Song, X., Li, Z., Li, Y., and Hou, H. (2022). Typical structure, biocompatibility, and cell proliferation bioactivity of collagen from Tilapia and Pacific cod. Colloids Surf. B Biointerfaces 210: 112238.

Suzuki, T., Takahashi, J., and Yamamoto, M. (2023). Molecular basis of the KEAP1-NRF2 signaling pathway. Mol. Cells 46(3): 133–141.

Ucak, I., Afreen, M., Montesano, D., Carrillo, C., Tomasevic, I., Simal-Gandara, J., and Barba, F.J. (2021). Functional and bioactive properties of peptides derived from marine side streams. Mar. Drugs 19(2): 71.

Uitto, J. (1997). Understanding premature skin aging. N. Engl. J. Med. 337(20): 1463–1465.

Wu, L., Hu, X., Xu, L., and Zhang, G. (2020). Cod skin oligopeptide inhibits human gastric carcinoma cell growth by inducing apoptosis. Nutr. Cancer 72(2): 218–225.

Wu, W., Li, B., Hou, H., Zhang, H., and Zhao, X. (2017). Isolation and identification of calcium-chelating peptides from Pacific cod skin gelatin and their binding properties with calcium. Food Funct. 8(12): 4441–4448.

Xiao, T., Chen, Y., Song, C., Xu, S., Lin, S., Li, M., Chen, X., and Gu, H. (2021). Possible treatment for UVB-induced skin injury: Anti-inflammatory and cytoprotective role of metformin in UVB-irradiated keratinocytes. J. Dermatol. Sci. 102(1): 25–35.

Yang, B., Li, Y., Guo, W., Zhang, Q., Pan, L., Duan, K., Zhang, P., Ren, L., Zhang, W., Wang, Q., and Kong, D. (2023). Optimized approach for active peptides identification in Cerebrolysin by nanoLC-MS. J. Chromatogr. B Analyt. Technol. Biomed. Life Sci. 1225: 123755.

Yuan, L., Duan, X., Zhang, R., Zhang, Y., and Qu, M. (2020). Aloe polysaccharide protects skin cells from UVB irradiation through Keap1/Nrf2/ARE signal pathway. J. Dermatolog. Treat. 31(3): 300–308.